HHS Public Access

Author manuscript

*J Invest Dermatol*. Author manuscript; available in PMC 2023 April 01.

Published in final edited form as:

*J Invest Dermatol*. 2022 April ; 142(4): 1085–1093. doi:10.1016/j.jid.2021.08.435.

# Functional Assessment of Missense Variants in the *ABCC6* gene Implicated in Pseudoxanthoma Elasticum, a Heritable Ectopic Mineralization Disorder

**Luke Kowal**[1,*], **Jianhe Huang**[1,*], **Hongbin Luo**[1,2], **Jagmohan Singh**[3], **Adam E. Snook**[3], **Jouni Uitto**[1], **Qiaoli Li**[1]

[1]Department of Dermatology and Cutaneous Biology, Sidney Kimmel Medical College, and PXE International Center of Excellence in Research and Clinical Care, Jefferson Institute of Molecular Medicine, Thomas Jefferson University, Philadelphia, PA 19107, USA

[2]Department of Dermatology, The First Affiliated Hospital of Zhejiang Chinese Medical University, Hangzhou 310006, China

[3]Department of Pharmacology and Experimental Therapeutics, Thomas Jefferson University, Philadelphia, Pennsylvania, PA 19107, USA

## Abstract

Pseudoxanthoma elasticum (PXE), a heritable multi-system ectopic mineralization disorder, is caused by inactivating mutations in the *ABCC6* gene. The encoded protein ABCC6, a transmembrane transporter, has a specialized efflux function in hepatocytes by contributing to plasma levels of PPi, a potent inhibitor of mineralization in soft connective tissues. Reduced plasma PPi levels underlie the ectopic mineralization in PXE. In this study, we characterized the pathogenicity of three human *ABCC6* missense variants using an adenovirus-mediated liver-specific ABCC6 transgene expression system in an *Abcc6*$^{-/-}$ mouse model of PXE. Variants p.L420V and p.R1064W were found benign as they had abundance and plasma membrane localization in hepatocytes similar to the wild-type human ABCC6 transgene, normalized plasma PPi levels and prevented mineralization in the dermal sheath of vibrissae in muzzle skin, a phenotypic hallmark in the *Abcc6*$^{-/-}$ mice. In contrast, p.S400F was shown to be pathogenic as it failed to normalize plasma PPi levels and had no effect on ectopic mineralization despite normal expression and proper localization in hepatocytes. These results demonstrated that adenovirus-mediated hepatic ABCC6 expression in *Abcc6*$^{-/-}$ mice can provide a model system to effectively

Correspondence should be addressed to Q.L. (Qiaoli.Li@jefferson.edu): Qiaoli Li, PhD, Department of Dermatology and Cutaneous Biology, Sidney Kimmel Medical College, PXE International Center of Excellence in Research and Clinical Care, Thomas Jefferson University, 233 S. 10th Street, Suite 431 BLSB, Philadelphia, Pennsylvania 19107, Qiaoli.Li@Jefferson.edu.

*Equal contribution

AUTHOR CONTRIBUTIONS

Conceptualization: QL and JU; Funding Acquisition: QL and JU; Data Curation and Formal Analysis: LK, JH, HL, JS, AS, and QL; Supervision: QL; Writing – Original Draft and Preparation: QL; Writing – Review and Editing: LK, JH, HL, JS, AS, JU, and QL.



CONFLICT OF INTEREST

The authors state no conflict of interest.

elucidate the multifaceted functional consequences of human *ABCC6* missense variants identified in patients with PXE.

**Keywords**

Pseudoxanthoma elasticum; ectopic mineralization; missense variants; mouse model; protein replacement

## INTRODUCTION

The *ABCC6* gene encodes the putative transmembrane efflux transporter ABCC6 which is predominantly expressed in hepatocytes. Loss-of-function mutations in *ABCC6* result in pseudoxanthoma elasticum (PXE), a late onset ectopic mineralization disorder, with clinical manifestations in the skin, eyes, and cardiovascular system (Bergen et al., 2000, Le Saux et al., 2000, Ringpfeil et al., 2000). Inactivating mutations in *ABCC6* can also cause generalized arterial calcification of infancy (GACI type II), an early onset and severe vascular calcification disorder in infants (Li et al., 2014, Nitschke et al., 2012). The lack of ABCC6 expression in clinically affected tissues suggests the long-range effects of the transporter in the liver. While the substrate of ABCC6 remains unknown, early studies demonstrated that PXE is a metabolic disorder caused by defective ABCC6 transport activity in the liver resulting in reduced circulating levels of an anti-calcifying factor, placing ABCC6 at a pivotal role in the regulation of connective tissue mineralization (Jiang et al., 2009). Recent data demonstrated that hepatic ABCC6 facilitates the extracellular release of adenosine triphosphate (ATP) which provides a crucial source of systemic inorganic pyrophosphate (PPi), a potent endogenous mineralization inhibitor (Jansen et al., 2014, Jansen et al., 2013). The role of ABCC6-mediated ATP release was supported by the observations of reduced levels of PPi in the plasma of *Abcc6*$^{-/-}$ mice and rats as well as in patients with PXE (Jansen et al., 2014, Li et al., 2019, Li et al., 2017). Thus, absence of ABCC6-dependent ATP release and reduced plasma PPi levels are critical pathogenic features of PXE.

To date, more than 300 distinct variants in the *ABCC6* gene have been identified in PXE patients, however, the pathogenicity of many of these variants is unclear (Luo et al., 2020). With the exception of p.R1141* and del23-29, two predominant recurrent pathogenic variants in *ABCC6*, all other variants are rare and private often limited to a single family or individual, and consequently, traditional approaches to establish pathogenicity, such as variant segregation within a pedigree or identification of independent families, are infeasible.

Missense variants are the most frequent and account for more than 50% of all types of variants in *ABCC6* (Legrand et al., 2017, Li et al., 2009). The annotation of missense variants has primarily relied on the predictions by *in silico* algorithms. However, these programs do not often provide consistent predictions. In addition, many of them are classified as variants of unknown significance (VUS), posing a huge dilemma in genetic counselling (Verschuere et al., 2021). Due to the metabolic nature of PXE and the biological role of hepatic ABCC6 in systemic PPi homeostasis, the establishment of the link between

ABCC6 functionality in the liver and mineralization in distal tissues requires specialized assays. In this study, we experimentally assessed the outcomes of three human *ABCC6* missense variants, p.S400F, p.L420V, and p.R1064W, for which *in silico* predictions are uncertain. Utilizing an *Abcc6*$^{-/-}$ mouse model of PXE (Klement et al., 2005), the pathogenicity of these variants was assessed for the abundance and localization of their corresponding mutant proteins, as well as plasma PPi levels and the extent of tissue mineralization. The adenovirus-mediated liver-specific human ABCC6 transgene expression system provided a useful approach to determine whether a missense variant in *ABCC6* is disease-associated.

## RESULTS

### *In silico* predictions of the pathogenicity of human *ABCC6* missense variants

A number of computational programs with different algorithms and metrics were used to predict the pathogenicity of three human *ABCC6* missense variants, p.S400F, p.L420V, and p.R1064W (Table 1). First, p.S400F and p.L420V are rare with a minor allele frequency (MAF) < 0.005% in the ExAC and gnomAD general population databases. In contrast, p.R1064W has a high MAF of 2% with 86 healthy individuals homozygous for this sequence variant. Second, we analyzed the predictions of these variants from Franklin which lists over ten different prediction algorithms including MutationTaster, PolyPhen-2, and Sift, which are commonly used to predict whether a variant affects the function of the protein. The aggregated prediction is disease-causing for all three variants although discrepancies occur among these algorithms. Third, p.S400F and p.L420V are classified as variants of unknown significance (VUS) and 3-U (3-unknown) following the latest guidelines set forth by the American College of Medical Genetics and Genomics/Association for Molecular Pathology (ACMG/AMP) and Sherloc, respectively (Nykamp et al., 2017, Richards et al., 2015). ACMG/AMP classifies p.R1064W as pathogenic (P), however, Sherloc annotates it as benign (1-B). Lastly, the damaging score of each variant was calculated using the Combined Annotation–Dependent Depletion (CADD), a recently developed method combining more than 60 diverse annotations into a single measure (CADD score) (Kircher et al., 2014, Rentzsch et al., 2019). While the program does not declare a single universal cut-off value, a score of 20 and 10 indicates the variants are among the top 1% and 10%, respectively, most deleterious to the human genome. The uncertainty and inconsistency of current predictions prompted us to investigate the pathogenicity of these missense variants *in vitro* and in an *ABCC6* gene-specific experimental system *in vivo*.

### *In vitro* characterization of human *ABCC6* missense variants

To determine whether missense variants affect expression of the mutant ABCC6 protein, adenovirus vectors carrying either wild-type (WT) human *ABCC6* cDNA or variant p.S400F, p.L420V, and p.R1064W, were generated and transduced into mouse liver hepatoma cells at different multiplicities of infection (MOI). Transduced cells demonstrated dose-dependent expression of WT and mutant human ABCC6 proteins (Figure 1).

### *In vivo* characterization of human *ABCC6* missense variants

Recombinant adenovirus carrying human *ABCC6* cDNA, either WT or p.S400F, p.L420V and p.R1064W, was administered intravenously to *Abcc6*$^{-/-}$ mice on *Rag1*$^{-/-}$ immunodeficient background (Huang et al., 2019). Injection of the adenoviruses were initiated in these mice at six weeks of age, a time point of the earliest stages of ectopic mineralization (Klement et al., 2005). Each mouse received 4x10$^{8}$ infectious unit (IFU), the same dose that was shown to normalize plasma PPi levels by the WT human ABCC6 protein (Huang et al., 2019). One week after injection, some of these mice were euthanized and their livers were collected for the determination of ABCC6 expression by immunostaining with an antibody against human ABCC6. The abundance of all three ABCC6 mutant proteins was indistinguishable from the WT human ABCC6 protein (data not shown). As missense variants may affect protein stability due to alterations in intracellular trafficking, the abundance and localization of the corresponding mutant ABCC6 proteins was also analyzed four weeks after injection (Figure 2). The levels of mutant human ABCC6 proteins were sustained up to four weeks, similar to the WT protein. In addition, dual immunostaining with antibodies against human ABCC6 and Na,K-ATPase, a plasma membrane marker at the basolateral side of hepatocytes, demonstrated co-localization for WT and all three ABCC6 mutants (Figure 2). To further quantify human ABCC6 at the protein level, Western blot was performed with total proteins extracted from mouse livers. The *Abcc6*$^{-/-}$*Rag1*$^{-/-}$ mice, four weeks after injection of recombinant adenoviruses, showed levels of ABCC6 which correlated with immuno-labeling of liver tissues from these mice (Figure 3).

The outcome measures of plasma PPi levels and the degree of ectopic mineralization were evaluated in these mice four weeks after injection, at ten weeks of age (Figure 4). The results corroborated our early finding that the WT human ABCC6 protein restored plasma PPi level in the *Abcc6*$^{-/-}$*Rag1*$^{-/-}$ mice to that in WT mice (Figure 4b), suggesting that the reconstituted human ABCC6 protein compensated for the loss of the endogenous mouse protein by contributing PPi from the liver to the circulation. The degree of mineralization of the dermal sheath of vibrissae in the muzzle skin, an early and reliable biomarker in the overall mineralization process in *Abcc6*$^{-/-}$*Rag1*$^{-/-}$ mice, was examined by two independent assays. One piece of muzzle skin was processed for histopathological evaluation. Another piece of muzzle skin was quantified for the calcium content. A mineralization-specific stain, von Kossa, showed robust mineralization in the dermal sheath of vibrissae in the uninjected *Abcc6*$^{-/-}$*Rag1*$^{-/-}$ control mice or mice administered with a promoterless vector (PL) (Figure 4a). The *Abcc6*$^{-/-}$*Rag1*$^{-/-}$ mice receiving adenovirus carrying WT human *ABCC6* cDNA showed little, if any, ectopic mineralization in the muzzle skin (Figure 4a), with the calcium content indistinguishable from those in WT mice negative for ectopic mineralization (Figure 4c).

Plasma PPi levels in mice expressing p.L420V and p.R1064W mutant proteins were similar to the WT mice or *Abcc6*$^{-/-}$*Rag1*$^{-/-}$ mice expressing the WT human ABCC6 protein (Figure 4b). Consequently these mice did not develop ectopic mineralization (Figure 4a,c). In contrast, p.S400F mutant failed to normalize plasma PPi levels and did not prevent ectopic mineralization in *Abcc6*$^{-/-}$*Rag1*$^{-/-}$ mice (Figure 4). These results suggest that

p.L420V and p.R1064W are benign variants while p.S400F is a pathogenic variant in *ABCC6*.

### Comparison of bioinformatics predictions with the experimental results

Although predicted to be disease-causing (aggregated outcome) with a high CADD score over 20, yet with conflicting ACMG/AMP and Sherloc classifications (Table 1), the p.R1064W variant was shown to be benign in this functional study. While the CADD score is modest (12.75), but predicted to be VUS by ACMG/AMP and 3-U by Sherloc, p.L420V was found to be benign as well. In contrast, variant p.S400F with ACMG/AMP and Sherloc classifications as VUS and 3-U, respectively, CADD score over 30, our functional study suggests it is pathogenic. The discrepancy between bioinformatics predictions was also highlighted when PopViz, a recently developed program to allow a quantitative gene-centric prediction (Zhang et al., 2018), was used to categorize these variants (Figure 5). The CADD score of mutation significance cutoff (MCS) for the *ABCC6* gene with 95% confidence interval is 4.327, suggesting that variants with CADD score over 4.327 are more likely intolerant (Itan et al., 2016). Using this gene-specific score of 4.327 and recommended MAF of 0.00418 as thresholds, p.S400F and p.L420V (MAF < 0.00418 and CADD score > 4.327) are regarded as likely pathogenic or pathogenic while the pathogenicity of p.R1064W (MAF > 0.00418 and CADD score > 4.327) is less certain. Our functional studies provided compelling results that p.S400F is pathogenic, and that p.L420V and p.R1064W are benign.

## DISCUSSION

It has been a dilemma concerning the connection between mutations in the *ABCC6* gene, expressed primarily in the liver, and ectopic mineralization in the skin, eyes, and the arterial blood vessels of peripheral tissues. PXE is determined to be a metabolic disorder resulting from hepatic ABCC6-dependent transporter defect leading to reduced concentration of a circulating anti-calcifying factor (Jiang et al., 2009). It was later discovered that hepatic ABCC6 promotes ATP externalization toward extracellular milieu, albeit with an unknown mechanism (Jansen et al., 2014, Jansen et al., 2013). ATP is rapidly transformed by ENPP1, an ectonucleotide pyrophosphatase/phosphodiesterase providing PPi in the circulation. PPi, a source of cell energy, is also an important circulating and tissue anti-calcifying factor. Micromolar concentration of PPi is sufficient to inhibit the deposition of hydroxyapatite crystals in the connective tissues in the presence of millimolar concentration of phosphate and calcium (Fleisch et al., 1966). ABCC6-dependent PPi deficiency is a major determinant of ectopic mineralization in PXE.

While significant progress has been made in understanding of the pathomechanisms of PXE, the pathogenicity of *ABCC6* variants that continue to be identified in patients with PXE, are largely uncharacterized. The majority of variants in *ABCC6* are missense variants. The ideal method to determine whether a suspected missense variant impairs protein abundance and cellular localization is to analyze the protein in the relevant tissues from individuals carrying the variants. However, this approach has significant limitations for *ABCC6* variants due to the metabolic nature of PXE. It is impossible to obtain liver biopsies from individuals carrying these variants, as liver is the organ that expresses ABCC6 (Belinsky and Kruh,

1999, Scheffer et al., 2002). A few functional studies attempted to examine a few human *ABCC6* missense variants in experimental settings (Jin et al., 2015, Le Saux et al., 2011, Pomozi et al., 2014). These studies analyzed the subcellular localization of the mutant human ABCC6 protein in transfected MDCKII (Madin-Darby canine kidney) cells, and in mouse liver by transient expression of the mutant proteins via hydrodynamic tail vein injection of plasmid DNA. The abundance of the mutant protein, a fundamental property that underlies the function of a protein, was not analyzed in these studies. In addition, the transport activity of mutant ABCC6 was analyzed in Sf9 insect cells using glutathione-conjugated N-ethylmaleimide and Leukotriene C4 as artificial substrates (Le Saux et al., 2011). A zebrafish embryo system was used to evaluate whether the mutant human *ABCC6* mRNA could rescue the *abcc6* morpholino-induced developmental phenotype (Li et al., 2010). Transduction of hepatocytes by hydrodynamic tail vein injection with plasmid DNA provided only a transient, up to several days with low-level expression of ABCC6 in mouse liver. Consequently, long-term evaluation of the ABCC6-dependent PPi levels in plasma and ectopic mineralization of connective tissues was impossible. Thus, we developed a liver-specific system with high and sustained ABCC6 transgene expression to objectively evaluate the pathogenicity of human *ABCC6* missense variants in a mouse model of PXE which recapitulates the histopathologic and clinical features of human PXE.

In this study, we took advantage of the adenovirus-mediated liver-specific human ABCC6 transgene expression in the $Abcc6^{-/-}Rag1^{-/-}$ mouse model of PXE. This approach allows us not only to evaluate the abundance and subcellular localization of the mutant human ABCC6 protein but also to examine the downstream functional consequences of plasma PPi levels and spontaneous ectopic mineralization. The experimental results reconciled the discrepancy of bioinformatics predictions, including the use of *ABCC6* gene-level thresholds for variant-level predictions (Itan et al., 2016). Of many available human *ABCC6* missense variants, these three variants were chosen as they are classified as VUS or with conflicting predictions. It should be noted that while refinement of VUS using Sherloc increases the number of likely pathogenic and pathogenic *ABCC6* missense variants, a significant number of variants still remain as VUS, as is the case for p.S400F and p.L420V (Verschuere et al., 2021). Variant p.R1064W was reported in several independent studies to be a pathogenic variant in patients with PXE (Hosen et al., 2015, Hosen et al., 2014, Miksch et al., 2005). However, our functional assessment of this variant suggests it is benign.

One of the limitations of the study relates to the use of the human *ABCC6* cDNA (~4.5 Kb) instead of genomic DNA (~75 Kb) in the adenovirus vector. As such, the variants are not in their native *ABCC6* gene structure. In addition, the expression of the human *ABCC6* transgene in mice may not fully reflect the functionality of this protein in human. While the *in silico* bioinformatics analyses can only provide a supporting criteria for sequence variants, our *in vivo* trans-species mouse model system has similar limitations. Therefore, the variant-associated clinical decision-making should be made with caution. Finally, the natural substrate of ABCC6 has not been identified. Plasma PPi was used as a surrogate marker of ABCC6 transport activity in the liver. However, our prior studies suggested that PPi deficiency is the major but possibly not the only cause in PXE; additional, yet unidentified tissue-specific factors might play a role (Zhao et al., 2017). Nevertheless, the

analysis of the ultimate ectopic mineralization in the mouse model bridges the gap between a not fully-understood hepatic transporter and the clinical phenotypes in distant tissues.

In conclusion, we show that adenovirus-mediated liver-specific human ABCC6 protein replacement in an ABCC6-deficient mouse model of PXE represents a useful and relevant model system to evaluate the functional consequences of *ABCC6* missense variants. Pathogenic variants in *ABCC6* can cause both PXE and GACI type II, two clinical entities at the two ends of a clinical spectrum of ectopic tissue mineralization (Luo et al., 2020). Solely relying on bioinformatics predictions will result in mis-classification of the variants, hampering clinical diagnosis and presymptomatic testing in individuals with family history of PXE and GACI type II. In the next-generation sequencing era, with a large number of variants being identified, their functional characterization in appropriate model systems is of paramount importance towards unambiguous annotations.

## MATERIALS AND METHODS

### Bioinformatics analysis

Recommendations of the Human Genome Variation Society (http://www.hgvs.org/mutnomen/) were followed for variant nomenclature. The +1 corresponds to the A nucleotide in the ATG translation initiation codon of the *ABCC6* reference sequence (GeneBank accession no. NM_001171.5). The allele frequency in the general population was extracted from Exome Aggregation Consortium (ExAC) (ExAC.BroadInstitute.org) and Genome Aggregation Database (gnomAD) (gnomad.broadinstitute.org) consisting of over 60,000 and 120,000 unrelated healthy individuals, respectively, sequenced in population genetic studies. Various *in silico* prediction programs with different metrics were used to assess the effect of variants on possible changes in the protein function (https://franklin.genoox.com/clinical-db/home). Classification of variants follows the guidelines of the latest American College of Medical Genetics and Genomics/Association for Molecular Pathology (ACMG/AMP), and Sherloc version 4.2 (Nykamp et al., 2017, Richards et al., 2015). ACMG/AMP classifies variants as benign (B), likely benign (LB), variants of unknown significance (VUS), likely pathogenic (LP), and pathogenic (P). Sherloc further refines the classification using a semi-quantitative 0-5 scoring system: number 5 denotes the evidence being “very high” and number 0 denotes the evidence being “low”. In addition, the Combined Annotation Depletion score (CADD) was used to assess the deleteriousness of sequence variants (https://cadd.gs.washington.edu/) (Kircher et al., 2014, Rentzsch et al., 2019).

The *ABCC6* gene-centric prediction of sequence variants was performed by plotting the CADD score versus the minor allele frequency (MAF) for each variant using PopViz server (Zhang et al., 2018). The *ABCC6*-gene specific mutation significance cut-off (MCS) within the 95% confidence interval and the recommended threshold for minor allele frequency (MAF) were calculated using the MCS method (Itan et al., 2016).

### Vector design and manufacturing

Human *ABCC6* coding sequence (NP_001162.4) was cloned into pENTR™/D-TOPO vector (Life Technologies, Grand Island, NY). Constructs with individual missense variants were generated using the Quick Change XL site-directed mutagenesis kit (Stratagene, La Jolla, CA), according to the manufacturer's instructions. To avoid nucleotide errors introduced during mutagenesis, the full-length *ABCC6* cDNAs were sequenced (GenScript, New Brunswick, NJ). The wild-type or mutant *ABCC6* cDNAs were recombined into the E1 region of the pAd/CMV/V5-DEST vector (Thermo Fisher, Grand Island, NY) containing E1- and E3-deleted human adenovirus serotype 5 (Ad5), as described previously (Huang et al., 2019).

### *In vitro* transduction

The mouse liver hepatoma cells (ATCC, Manassas, VA) were transduced with recombinant adenoviruses carrying wild-type or mutant *ABCC6* cDNAs at different multiplicities of infection (MOI). Human ABCC6 expression were detected 36 hours post transduction by immunostaining using human ABCC6-specific antibody M6II-7 (Cell Sciences, Newburyport, MA), as previously described (Huang et al., 2019). The transduction efficiency was quantified by the percentage of positively stained cells.

### Mice and injections

The *Abcc6*$^{tm1JfK}$ mouse was described previously and referred to as *Abcc6*$^{-/-}$ (Klement et al., 2005). The *Abcc6*$^{-/-}$ mice on immunodeficient *Rag1*$^{tm1Mom/J}$ mouse background (referred to as *Rag1*$^{-/-}$) (The Jackson Laboratory, Bar Harbor, ME) were used to test the pathogenicity of *ABCC6* missense variants. In all groups, six-week-old *Abcc6*$^{-/-}$*Rag1*$^{-/-}$ mice were intravenously injected with recombinant adenoviruses at $4x10^8$ IFU per mouse. Mice were euthanized one and four weeks afterwards. All mice, including the wild-type (WT) C57BL/6J mice and the *Abcc6*$^{-/-}$*Rag1*$^{-/-}$ mice congenic on the C57BL/6J background, were maintained on a standard rodent diet. All protocols were approved by the Institutional Animal Care and Use Committee of Thomas Jefferson University.

### Immunostaining of the human ABCC6 protein

Immunostaining of liver was performed on 6 μm frozen sections. The rat monoclonal anti-human ABCC6 antibody M6II-7 (Cell Sciences), 1:100 dilution, was used to identify the human ABCC6 protein. A mouse monoclonal antibody, 1:100 dilution, was used to label the basolateral plasma membrane marker Na,K-ATPase (Abcam, Cambridge, MA). The Alexa Fluor 488 donkey anti-rat and Alexa Fluor 594 goat anti-mouse secondary antibodies (Life Technologies), both at 1:400 dilution, were used. Primary and secondary antibodies were incubated at 4°C overnight and at room temperature for 1 hour, respectively. Images were acquired using A1R+ Nikon confocal microscope (Nikon Instruments Inc., Melville, NY).

### Western blot

Total proteins from mouse liver were prepared and separated on 8% SDS-PAGE. An anti-ABCC6 antibody M6II-7 (Cell Sciences), 1:500, was used to detect the human ABCC6 protein. A mouse monoclonal anti Na,K-ATPase antibody, 1:500, was used as a plasma

membrane marker for equal protein loading. The membrane was incubated with secondary antibodies, 1:20,000, and scanned with an Odyssey Infrared Imager (LI-COR Biosciences, Lincoln, NE). The bands were quantified by densitometry using the LI-COR software.

### Histopathological analysis

Left muzzle skin biopsies from euthanized mice were collected and processed for histopathology. Paraffin sections were examined for calcification by von Kossa staining (American Mastertech Scientific, Inc., Lodi, CA).

### Chemical quantitation of calcium

Right muzzle skin biopsies were decalcified in 250 μL 1.0 mol/L HCl for 48 hours at room temperature. Solubilized calcium was determined using a colorimetric assay kit (Stanbio Laboratory, Boerne, TX). The values were normalized to tissue weight.

### Plasma collection and PPi assay

Whole blood was collected by cardiac puncture and determination of PPi concentration in plasma was performed as previously described (Huang et al., 2019).

### Statistical analysis

The data were analyzed using multivariable linear regression with multiple group comparison corrections. Statistical significance was reached with $P < 0.05$. All statistical analyses were completed using Prism 8 (GraphPad, San Diego, CA).

## ACKNOWLEDGMENTS

This study was supported by PXE International, NIH/NIAMS grants R01AR072695 (JU and QL) and R21AR077332 (QL). The authors thank Ida Joely Jacobs, Douglas Ralph, Amir Hossein Saeidian, Leila Youssefian and Hassan Vahidnezhad for assistance.

## DATA AVAILABILITY STATEMENT

All data associated with this study are presented in the paper.

## Abbreviations:

| | |
|---|---|
| **Ad5** | adenovirus serotype 5 |
| **PXE** | pseudoxanthoma elasticum |
| **GACI** | generalized arterial calcification of infancy |
| **PPi** | inorganic pyrophosphate |
| **WT** | wild-type |
| **KO** | knockout |

## REFERENCES


Belinsky MG, Kruh GD. MOAT-E (ARA) is a full-length MRP/cMOAT subfamily transporter expressed in kidney and liver. Br J Cancer 1999;80(9):1342–9. [PubMed: 10424734]

Bergen AA, Plomp AS, Schuurman EJ, Terry S, Breuning M, Dauwerse H, et al. . Mutations in ABCC6 cause pseudoxanthoma elasticum. Nat Genet 2000;25(2):228–31. [PubMed: 10835643]

Fleisch H, Russell RG, Straumann F. Effect of pyrophosphate on hydroxyapatite and its implications in calcium homeostasis. Nature 1966;212(5065):901–3. [PubMed: 4306793]

Hosen MJ, Van Nieuwerburgh F, Steyaert W, Deforce D, Martin L, Leftheriotis G, et al. . Efficiency of exome sequencing for the molecular diagnosis of pseudoxanthoma elasticum. J Invest Dermatol 2015;135(4):992–8. [PubMed: 25264593]

Hosen MJ, Zubaer A, Thapa S, Khadka B, De Paepe A, Vanakker OM. Molecular docking simulations provide insights in the substrate binding sites and possible substrates of the ABCC6 transporter. PLoS One 2014;9(7):e102779. [PubMed: 25062064]

Huang J, Snook AE, Uitto J, Li Q. Adenovirus-Mediated ABCC6 Gene Therapy for Heritable Ectopic Mineralization Disorders. J Invest Dermatol 2019;139(6):1254–63. [PubMed: 30639429]

Itan Y, Shang L, Boisson B, Ciancanelli MJ, Markle JG, Martinez-Barricarte R, et al. . The mutation significance cutoff: gene-level thresholds for variant predictions. Nat Methods 2016;13(2):109–10. [PubMed: 26820543]

Jansen RS, Duijst S, Mahakena S, Sommer D, Szeri F, Varadi A, et al. . ABCC6-mediated ATP secretion by the liver is the main source of the mineralization inhibitor inorganic pyrophosphate in the systemic circulation-brief report. Arterioscler Thromb Vasc Biol 2014;34(9):1985–9. [PubMed: 24969777]

Jansen RS, Kucukosmanoglu A, de Haas M, Sapthu S, Otero JA, Hegman IE, et al. . ABCC6 prevents ectopic mineralization seen in pseudoxanthoma elasticum by inducing cellular nucleotide release. Proc Natl Acad Sci U S A 2013;110(50):20206–11. [PubMed: 24277820]

Jiang Q, Endo M, Dibra F, Wang K, Uitto J. Pseudoxanthoma elasticum is a metabolic disease. J Invest Dermatol 2009;129(2):348–54. [PubMed: 18685618]

Jin L, Jiang Q, Wu Z, Shao C, Zhou Y, Yang L, et al. . Genetic heterogeneity of pseudoxanthoma elasticum: the Chinese signature profile of ABCC6 and ENPP1 mutations. J Invest Dermatol 2015;135(5):1294–302. [PubMed: 25615550]

Kircher M, Witten DM, Jain P, O'Roak BJ, Cooper GM, Shendure J. A general framework for estimating the relative pathogenicity of human genetic variants. Nat Genet 2014;46(3):310–5. [PubMed: 24487276]

Klement JF, Matsuzaki Y, Jiang QJ, Terlizzi J, Choi HY, Fujimoto N, et al. . Targeted ablation of the abcc6 gene results in ectopic mineralization of connective tissues. Mol Cell Biol 2005;25(18):8299–310. [PubMed: 16135817]

Le Saux O, Fulop K, Yamaguchi Y, Ilias A, Szabo Z, Brampton CN, et al. . Expression and in vivo rescue of human ABCC6 disease-causing mutants in mouse liver. PLoS One 2011;6(9):e24738. [PubMed: 21935449]

Le Saux O, Urban Z, Tschuch C, Csiszar K, Bacchelli B, Quaglino D, et al. . Mutations in a gene encoding an ABC transporter cause pseudoxanthoma elasticum. Nat Genet 2000;25(2):223–7. [PubMed: 10835642]

Legrand A, Cornez L, Samkari W, Mazzella JM, Venisse A, Boccio V, et al. . Mutation spectrum in the ABCC6 gene and genotype-phenotype correlations in a French cohort with pseudoxanthoma elasticum. Genet Med 2017;19(8):909–17. [PubMed: 28102862]

Li Q, Brodsky JL, Conlin LK, Pawel B, Glatz AC, Gafni RI, et al. . Mutations in the ABCC6 gene as a cause of generalized arterial calcification of infancy: genotypic overlap with pseudoxanthoma elasticum. J Invest Dermatol 2014;134(3):658–65. [PubMed: 24008425]

Li Q, Huang J, Pinkerton AB, Millan JL, van Zelst BD, Levine MA, et al. . Inhibition of Tissue-Nonspecific Alkaline Phosphatase Attenuates Ectopic Mineralization in the Abcc6(−/−) Mouse Model of PXE but Not in the Enpp1 Mutant Mouse Models of GACI. J Invest Dermatol 2019;139(2):360–8. [PubMed: 30130617]

Li Q, Jiang Q, Pfendner E, Varadi A, Uitto J. Pseudoxanthoma elasticum: clinical phenotypes, molecular genetics and putative pathomechanisms. Exp Dermatol 2009;18(1):1–11. [PubMed: 19054062]

Li Q, Kingman J, van de Wetering K, Tannouri S, Sundberg JP, Uitto J. Abcc6 Knockout Rat Model Highlights the Role of Liver in PPi Homeostasis in Pseudoxanthoma Elasticum. J Invest Dermatol 2017;137(5):1025–32. [PubMed: 28111129]

Li Q, Sadowski S, Frank M, Chai C, Varadi A, Ho SY, et al. . The abcc6a gene expression is required for normal zebrafish development. J Invest Dermatol 2010;130(11):2561–8. [PubMed: 20596085]

Luo H, Faghankhani M, Cao Y, Uitto J, Li Q. Molecular Genetics and Modifier Genes in Pseudoxanthoma Elasticum, a Heritable Multisystem Ectopic Mineralization Disorder. J Invest Dermatol 2020.

Miksch S, Lumsden A, Guenther UP, Foernzler D, Christen-Zach S, Daugherty C, et al. . Molecular genetics of pseudoxanthoma elasticum: type and frequency of mutations in ABCC6. Hum Mutat 2005;26(3):235–48. [PubMed: 16086317]

Nitschke Y, Baujat G, Botschen U, Wittkampf T, du Moulin M, Stella J, et al. . Generalized arterial calcification of infancy and pseudoxanthoma elasticum can be caused by mutations in either ENPP1 or ABCC6. Am J Hum Genet 2012;90(1):25–39. [PubMed: 22209248]

Nykamp K, Anderson M, Powers M, Garcia J, Herrera B, Ho YY, et al. . Sherloc: a comprehensive refinement of the ACMG-AMP variant classification criteria. Genet Med 2017;19(10):1105–17. [PubMed: 28492532]

Pomozi V, Brampton C, Fulop K, Chen LH, Apana A, Li Q, et al. . Analysis of pseudoxanthoma elasticum-causing missense mutants of ABCC6 in vivo; pharmacological correction of the mislocalized proteins. J Invest Dermatol 2014;134(4):946–53. [PubMed: 24352041]

Rentzsch P, Witten D, Cooper GM, Shendure J, Kircher M. CADD: predicting the deleteriousness of variants throughout the human genome. Nucleic Acids Res 2019;47(D1):D886–D94. [PubMed: 30371827]

Richards S, Aziz N, Bale S, Bick D, Das S, Gastier-Foster J, et al. . Standards and guidelines for the interpretation of sequence variants: a joint consensus recommendation of the American College of Medical Genetics and Genomics and the Association for Molecular Pathology. Genet Med 2015;17(5):405–24. [PubMed: 25741868]

Ringpfeil F, Lebwohl MG, Christiano AM, Uitto J. Pseudoxanthoma elasticum: mutations in the MRP6 gene encoding a transmembrane ATP-binding cassette (ABC) transporter. Proc Natl Acad Sci U S A 2000;97(11):6001–6. [PubMed: 10811882]

Scheffer GL, Hu X, Pijnenborg AC, Wijnholds J, Bergen AA, Scheper RJ. MRP6 (ABCC6) detection in normal human tissues and tumors. Lab Invest 2002;82(4):515–8. [PubMed: 11950908]

Verschuere S, Navassiolava N, Martin L, Nevalainen PI, Coucke PJ, Vanakker OM. Reassessment of causality of ABCC6 missense variants associated with pseudoxanthoma elasticum based on Sherloc. Genet Med 2021;23(1):131–9. [PubMed: 32873932]

Zhang P, Bigio B, Rapaport F, Zhang SY, Casanova JL, Abel L, et al. . PopViz: a webserver for visualizing minor allele frequencies and damage prediction scores of human genetic variations. Bioinformatics 2018;34(24):4307–9. [PubMed: 30535305]

Zhao J, Kingman J, Sundberg JP, Uitto J, Li Q. Plasma PPi Deficiency Is the Major, but Not the Exclusive, Cause of Ectopic Mineralization in an Abcc6(−/−) Mouse Model of PXE. J Invest Dermatol 2017;137(11):2336–43. [PubMed: 28652107]

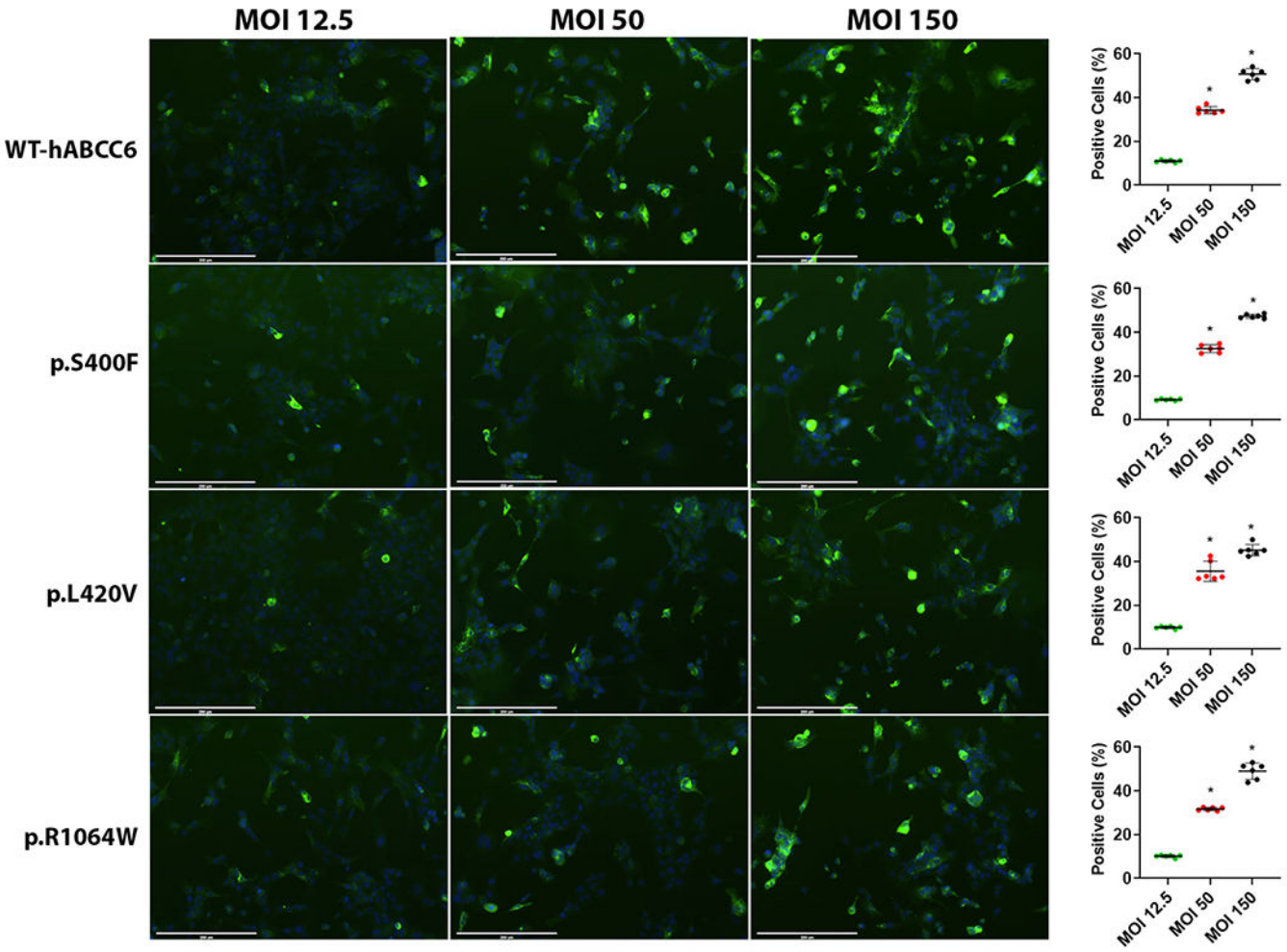


**Figure 1. Recombinant adenovirus transduction showed dose-dependent human ABCC6 protein expression *in vitro*.**

Mouse liver hepatoma cells were transduced with recombinant adenoviruses carrying either WT human *ABCC6* cDNA or missense variants (p.S400F, p.L420V, and p.R1064W) under the control of a CMV promoter. Cells were stained with a human ABCC6-specific antibody 36 hours after transduction. Dose-dependent human ABCC6 expression (Green fluorescence) was detected in cells transduced with recombinant adenoviruses at 12.5 to 100 MOI. Scale bars, 200 μm. Blue indicates DAPI staining of nuclei. The data were presented as mean ± SD. **P* < 0.01 compared with MOI 12.5 in each group. CMV, cytomegalovirus; MOI, multiplicity of infection; WT, wild-type.

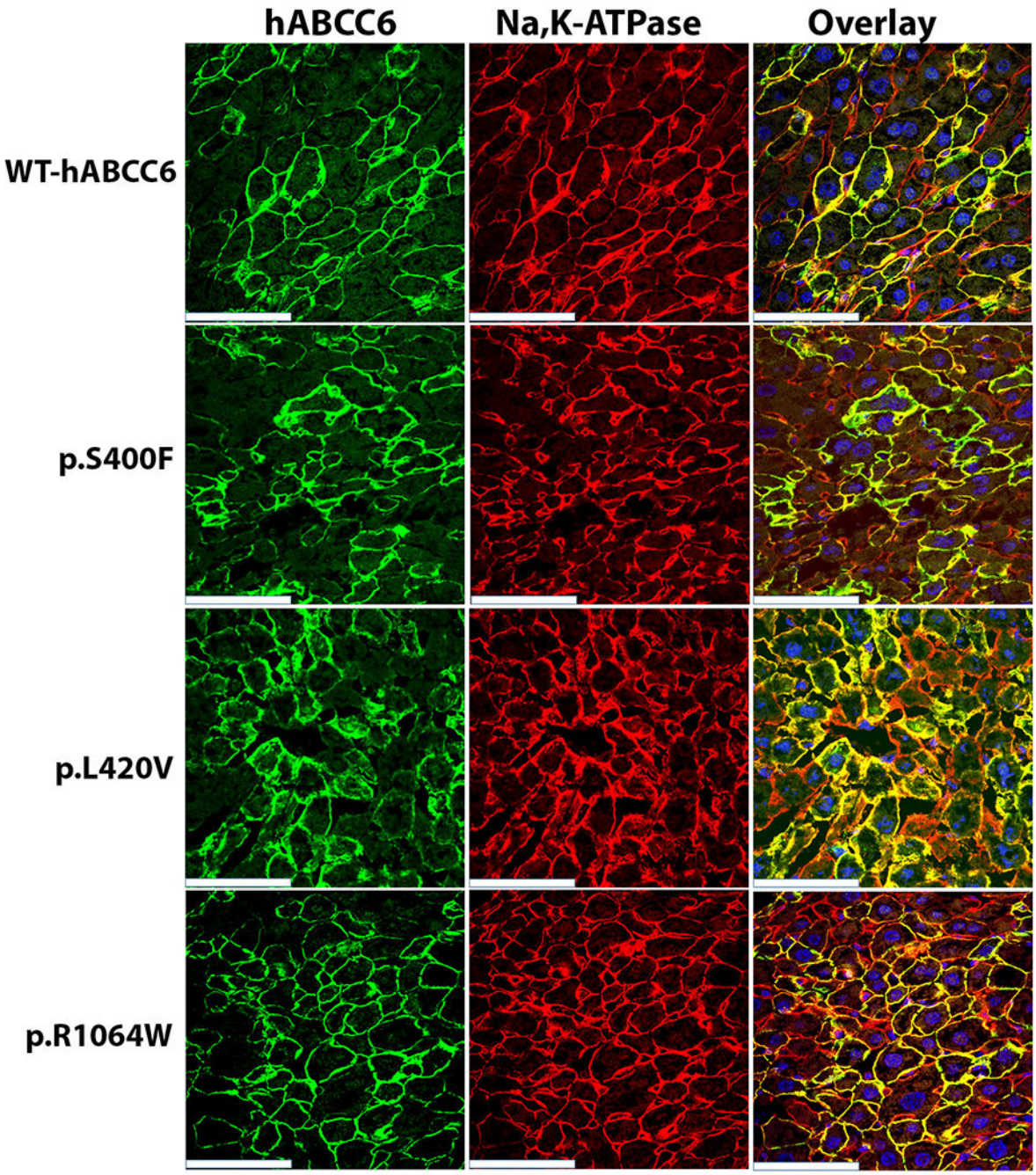


**Figure 2. Intravenous administration of recombinant adenovirus showed ABCC6 expression in the liver of *Abcc6*$^{-/-}$*Rag1*$^{-/-}$ mice.**

A group of 8-12 *Abcc6*$^{-/-}$*Rag1*$^{-/-}$ mice at 6 weeks of age were administered a single injection of 4x10$^{8}$ IFU recombinant adenoviruses carrying either WT human *ABCC6* cDNA or missense variants (p.S400F, p.L420V, and p.R1064W). The mice were analyzed at four weeks after injection. Immunostaining showed robust expression of human ABCC6 (Green fluorescence). Dual labeling with human ABCC6 (Green fluorescence) and Na,K-ATPase (Red fluorescence) showed co-localization in the basolateral plasma membrane of

hepatocytes for both WT and mutant proteins. Scale bars, 24 μm. Blue indicates DAPI staining of nuclei. IFU, infectious unit; WT, wild-type.

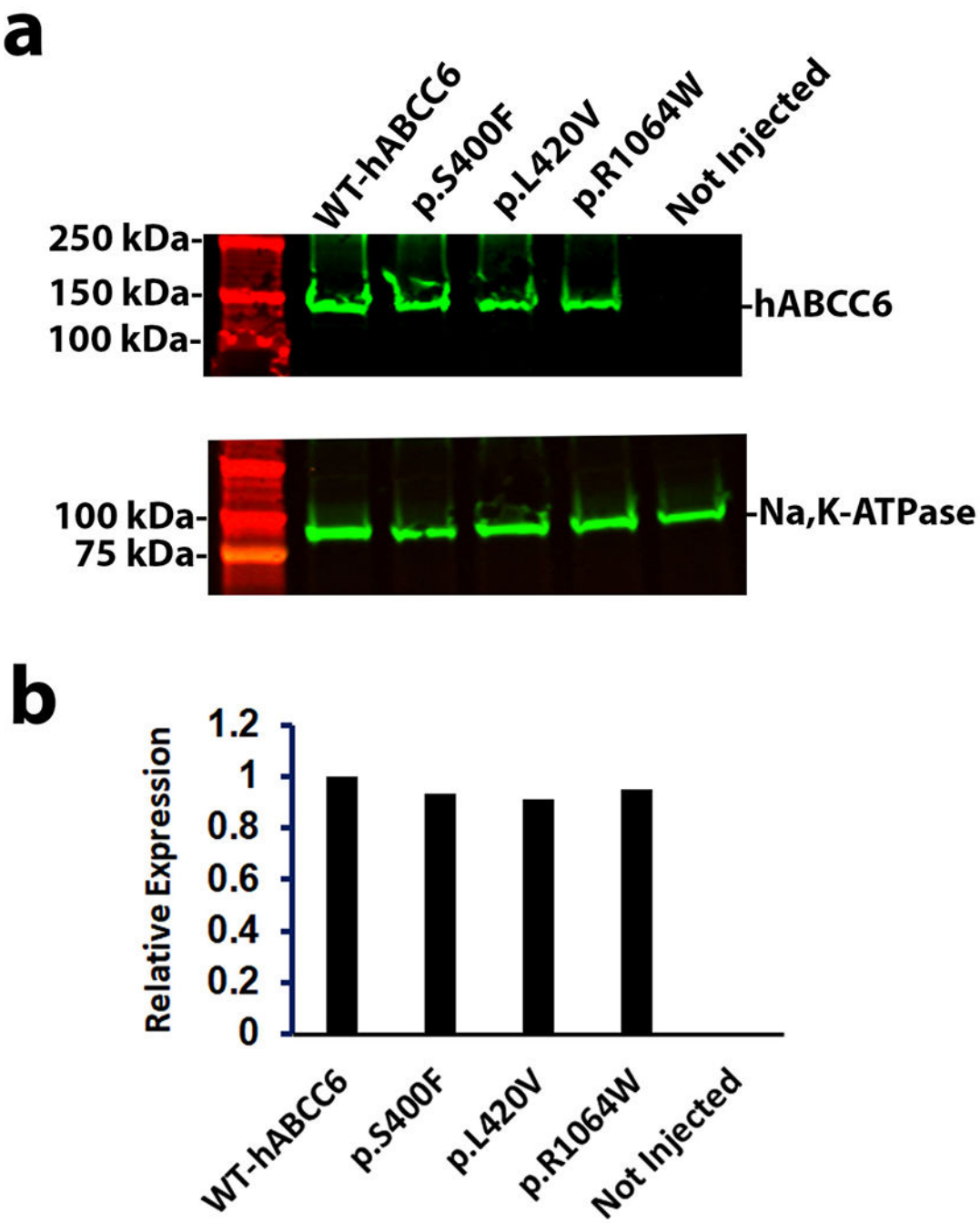


**Figure 3. Demonstration of human ABCC6 expression in mouse liver by Western blot.**

(**a**) Six-week-old *Abcc6*$^{-/-}$*Rag1*$^{-/-}$ mice received 4x10$^{8}$ IFU recombinant adenoviruses carrying either WT human *ABCC6* cDNA or missense variants (p.S400F, p.L420V, and p.R1064W) driven by a CMV promoter. ABCC6 expression in the liver was analyzed in these mice four weeks after injection, at ten weeks of age. The blot was stained with an anti-human ABCC6 antibody. A plasma membrane marker, Na,K-ATPase, served as internal loading control. Note the negative expression of human ABCC6 protein in the liver of uninjected *Abcc6*$^{-/-}$*Rag1*$^{-/-}$ mice. (**b**) Quantification of ABCC6 carrying p.S400F, p.L420V,

and p.R1064W by scanning densitometry, normalizing by their respective Na,K-ATPase, revealed that the corresponding ABCC6 abundance was 93%, 91%, and 95%, respectively, of the WT human ABCC6 protein. CMV, cytomegalovirus; IFU, infectious unit; WT, wild-type.

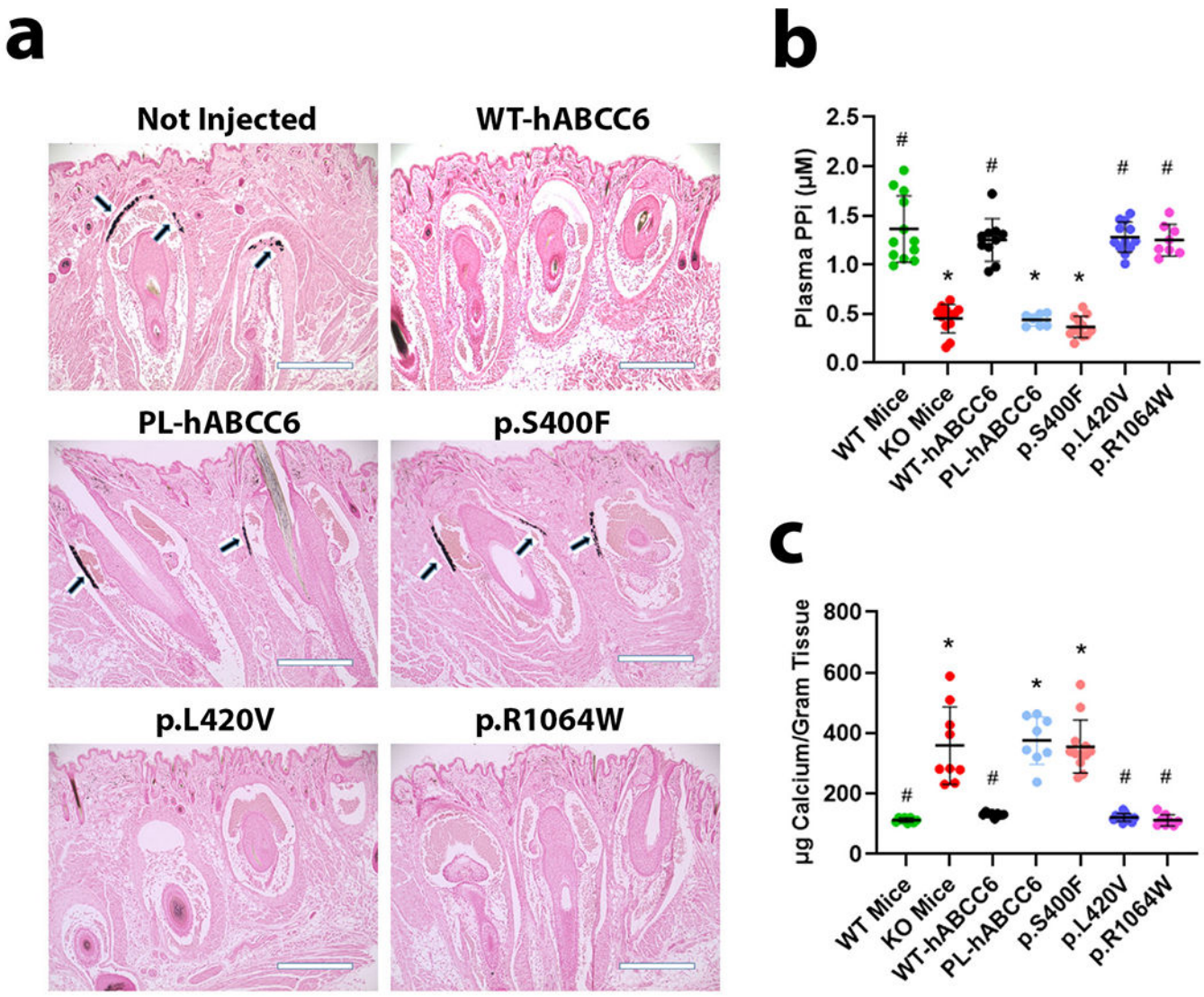


**Figure 4. Functional outcome measures of variants p.S400F, p.L420V, and p.R1064W.**

*Abcc6*$^{-/-}$*Rag1*$^{-/-}$ mice at six weeks of age received 4x10$^{8}$ IFU recombinant adenoviruses carrying either WT human *ABCC6* cDNA or missense variants (p.S400F, p.L420V, and p.R1064W) driven by a CMV promoter, or WT human *ABCC6* cDNA without a promoter (PL). The mice were analyzed four weeks after injection, at ten weeks of age. (**a**) Ectopic mineralization in the dermal sheath of vibrissae was analyzed by von Kossa histopathologic stains. Arrows indicate ectopic mineralization. Scale bars, 400 μm. (**b**) Plasma PPi levels. (**c**) The calcium content in the muzzle skin. The data were presented as mean ± SD. n= 8-12 mice per group. *$P < 0.01$ compared with WT control mice. $^{\#}P < 0.01$ compared with uninjected *Abcc6*$^{-/-}$*Rag1*$^{-/-}$ mice. CMV, cytomegalovirus; IFU, infectious unit; M, mol/L; PL, promoterless; PPi, inorganic pyrophosphate; WT, wild-type; KO, knockout.

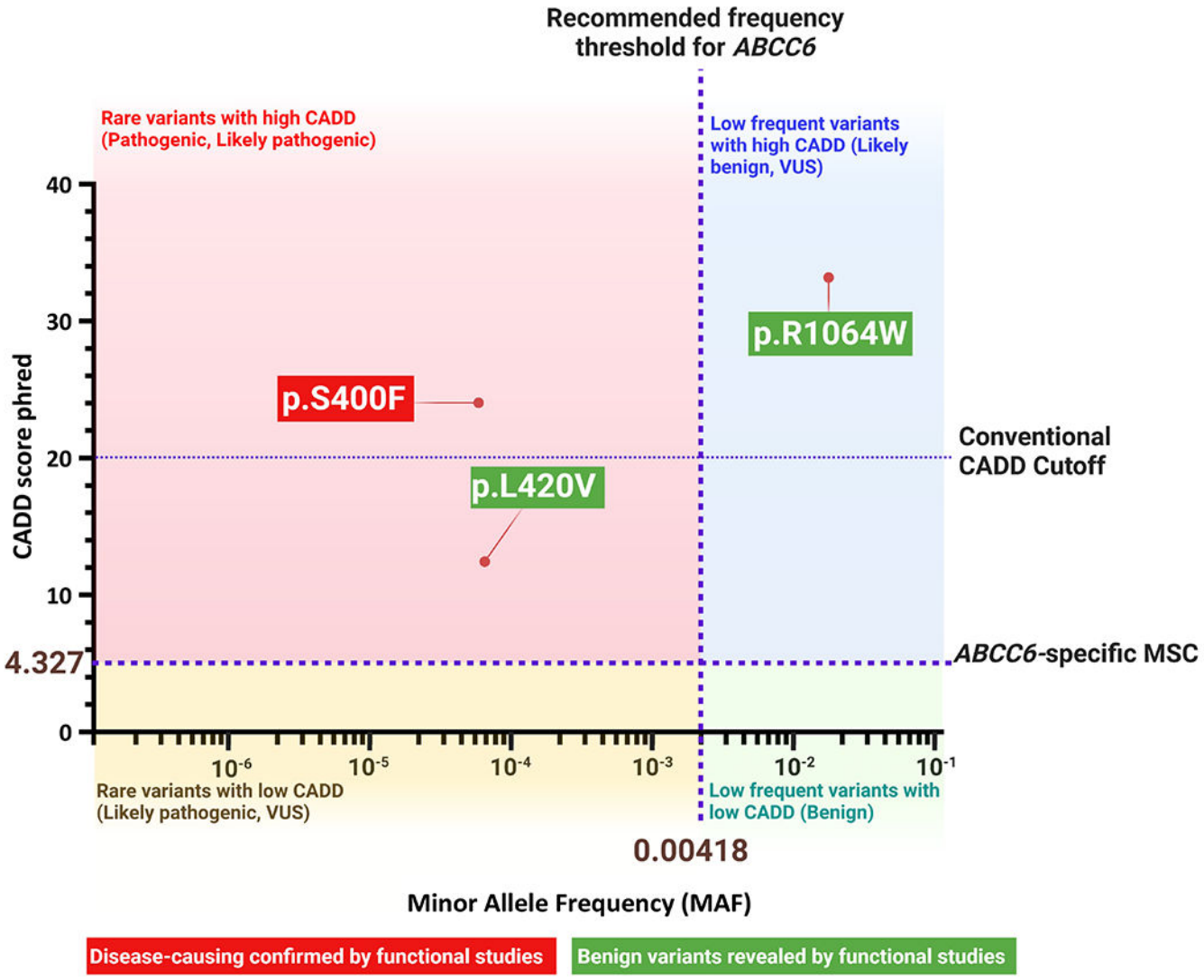


**Figure 5. The plot of CADD versus MAF of *ABCC6* variants p.S400F, p.L420V, and p.R1064W.**

While the conventional CADD score cutoff for a variant is 20 (dashed line), the *ABCC6* gene-specific mutation significance cutoff (MSC) with 95% confidence interval is 4.327 (thick dashed line). The recommended *ABCC6* gene-specific MAF threshold is 0.00418 (thick dashed line). MAF for each variant was obtained from gnomAD (aggregated; http://gnomad.broadinstitute.org, n = 125,748 exomes and 15,708 genomes). There are four groups of variants on the plot: 1) variants with CADD scores > 4.327 and MAF < 0.00418 (pink area, top left); 2) variants with CADD scores < 4.327 and MAF < 0.00418 (light yellow area, bottom left); 3) variants with CADD scores > 4.327 and MAF > 0.00418 (light blue, top right); 4) variants with CADD scores < 4.327 and MAF > 0.00418 (light green, bottom right).

**Table 1.**

*In silico* predictions of missense variants in the *ABCC6* gene and comparison with experimental results

| Variant[1)] | Bioinformatics analyses | | | | | | Experimental results | | | | |
|---|---|---|---|---|---|---|---|---|---|---|---|
| | Population data[2)]: No. of homozygous, MAF (%) | | Prediction outcome by | | | | ABCC6 expression (relative to WT-hABCC6 protein) | ABCC6 localization | Plasma PPi (relative to WT mice) | Ectopic mineralization (relative to KO mice) | Pathogenicity |
| | ExAC | gnomAD | Aggregated outcome[3)] | ACMG/AMP[4)] | Sherloc[5)] | CADD Score[6)] | | | | | |
| c.1199C>T, p.S400F | 0, 0.0043 | 0, 0.0027 | Disease causing | VUS | 3-U | 24.9 | ns | PM | Reduced, $P < 0.01$ | ns | Pathogenic |
| c.1258C>G, p.L420V | 0, 0.0027 | 0, 0.0025 | Disease causing | VUS | 3-U | 12.75 | ns | PM | ns | Reduced, $P < 0.01$ | Benign |
| c.3190C>T, p.R1064W | 39, 2.058 | 86, 2.0500 | Disease causing | P | 1-B | 33.0 | ns | PM | ns | Reduced, $P < 0.01$ | Benign |

1)Variant nomenclature was based on NG_007558.2 (NM_001171.5).

2)The Exome Aggregation Consortium (ExAC) and Genome Aggregation Database (gnomAD) consist of over 60,000 and 120,000 unrelated individuals sequenced in population genetic studies. The number of individuals carrying the specific variant as homozygous and the minor allele frequency (MAF) are provided.

3)While there are over ten different prediction algorithms, only the aggregated outcome is provided (https://franklin.genoox.com/clinical-db/home).

4)American College of Medical Genetics and Genomics/Association for Molecular Pathology (ACMG/AMP) classifies variants as benign (B), likely benign (LB), VUS (variants of unknown significance), likely pathogenic (LP), and pathogenic (P).

5)Sherloc further refines ACMG/AMP classifications using a semi-quantitative 0-5 numbering system. For each classification assigned by ACMG/AMP, number 5 denotes the evidence being “very high” and number 0 denotes the evidence being “low”. U, unknown.

6)The Combined Annotation Depletion score (CADD) score of 10 and 20 of a variant suggests the variant is among the top 10% and 1% most deleterious to the human genome, respectively.

ns, not significant; PM, plasma membrane; WT, wild-type; KO, *Abcc6*$^{-/-}$ knockout.